Operating Optically Current-Confined VCSELs With an External Laser Beam

Sven Bader and Mohamed Elattar

Optically controlled current confinement is an oxide- and regrowth-free method in vertical-cavity surface-emitting lasers (VCSELs) to funnel carriers in very close vicinity to the active layers to reach low lasing threshold currents. The essential component to steer the current flow through the laser is a monolithically integrated phototransistor (PT) in the cavity, operating as an optical switch. The PT layers become locally conductive where the highest photon density is reached in the resonator and establish the current aperture. Illuminating parts of the VCSEL by a focused external laser beam changes this spatial photon distribution by introducing additional photons. We demonstrate the possibility of manipulating the location of the current aperture as well as influencing the light–current characteristics by varying the power and wavelength of the external laser.

1. Introduction

Diverse novel fields of applications with the main scope of optical sensing and short-distance data communications have continuously increased the importance of vertical-cavity surface-emitting lasers in the past years [1]. However, not only the variety of applications contributed to the success but also profound VCSEL research and development played an important part. This resulted in more efficient, faster, and inexpensive lasers. Extending the device lifetime is a concern which is affected by several factors. One of them is the buried insulating oxide ring which funnels the current flow through its centered opening — the current aperture [2]. This leads to a strong local increase of current density and thus reduces the lasing threshold current. However, during the manufacture of this current aperture via selective wet-thermal oxidation, the high aluminum content AlGaAs layers of the top mirror reduce their volume when transformed to an oxide. Typically the current aperture is located close to the active zone. As a result, mechanical strain is directly transferred to the active layers of the VCSEL, which might affect the very-long-term reliability of the VCSEL [3]. Oxide-confined VCSELs are most popular for commercial use, however, alternative current confinement techniques like mesa-etching [4], proton implantation [5], or epitaxial regrowth [6, 7] still exist. Although the performance of those devices may be equivalent to that of oxidized VCSELs, the manufacturing effort is comparably high, in particular if regrowth is involved.

We have developed an optically controlled method for current confinement, where an epitaxially integrated phototransistor — configured as an optical switch — defines the current flow through the device [8]. The concept of this oxide- and regrowth-free approach

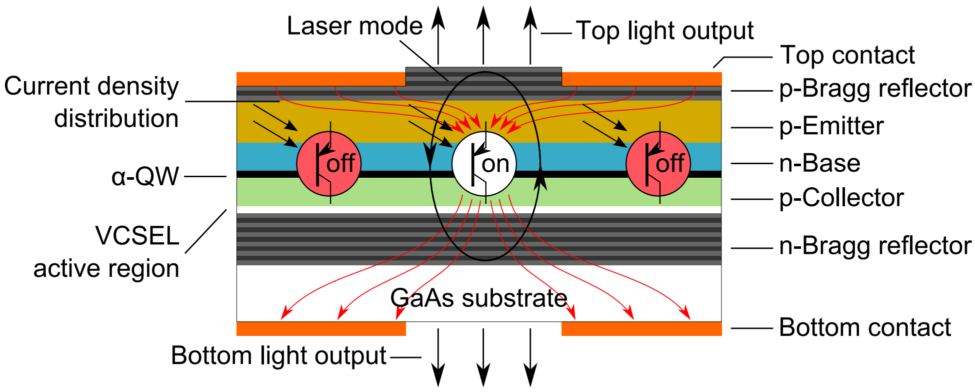

Fig. 1: Schematic layer structure of an optically current-confined VCSEL with integrated PT, which is configured as an optical switch. The PT opens where the highest lateral photon density is reached, thus the location of the current aperture strongly depends on the quality factor of the resonator and can be affected by etching the top mirror (i.e., under the top metal contact).

is discussed in detail in Sect. 2. The required photons for switching the PT conductive can either originate directly from the active zone of the PT-VCSEL or be injected into the resonator by an external laser beam. This new technique of defining and manipulating the current aperture is introduced in Sect. 3, where also its influence on the turn-on behavior of parallel-driven PT-VCSEL arrays will be investigated. Section 4 analyzes the impact of varying the output power and wavelength of the external laser on the light output curves of large-area VCSELs.

2. Optically Controlled Current Confinement

Optically current-confined PT-VCSELs combine the advantages of a strain-free epitaxial structure with a simple manufacturing process. Compared to existing methods, mentioned in Sect. 1, no physical barriers must be post-processed in order to partially block the current flow. Our approach epitaxially integrates a PT directly into the cavity where also the active zone of the VCSEL is located (see Fig. 1). As in a standard pnp-bipolar junction transistor configuration, the PT consists of p-emitter, n-base, and p-collector layers, however, except for the external base terminal. The base current I_{B} is generated in a dedicated quantum well (α-QW) between the base and collector layer by absorbing photons in the resonator. Actually, I_{B} is a photocurrent which can be calculated as

$$I_{\mathrm{B}} = (1 - \exp(-\alpha d)) \cdot \frac{q\lambda}{hc} \cdot P, \tag{1}$$

where α is the absorption coefficient and d is the width of the α-QW, q is the elementary charge, h is Planck's constant, and c the vacuum velocity of light with wavelength λ and optical power P in the cavity.

Ramping up the drive current, initially the PT acts as an insulating barrier which only allows leakage current to flow. However, this current already causes spontaneous emission, generated in the InGaAs QWs of the active zone. These photons get partly absorbed in

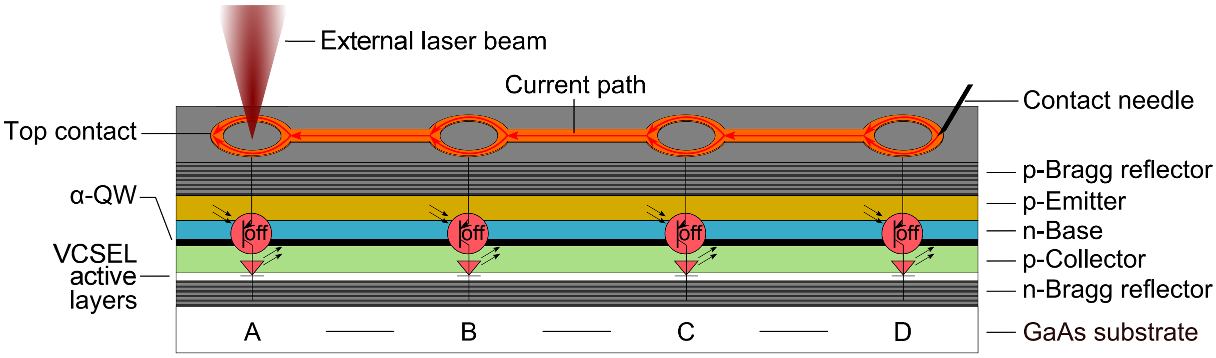

Fig. 2: Schematic layout of parallel-driven PT-VCSELs which are defined by four interconnected surface metal contact rings. The external laser beam is focused at position A and introduces additional photons in the resonator.

the α-QW and produce the base current (according to (1)). The GaAs-based PT-VCSEL is designed to absorb exclusively in the 1040 nm range via an InGaAs α-QW. Once I_B exceeds a certain threshold value, which mainly depends on the current gain, the lateral region of the PT with the highest photon density switches into a conductive state. The drive current now funnels through this current aperture, generates more photons and keeps this PT area open and stable in diameter. After reaching the threshold current density, the PT-VCSEL starts lasing. The location of the current aperture strongly depends on the spatial photon density during the turn-on of the device. It can either be influenced by the quality factor of the resonator, determined by, e.g., the number of top mirror pairs (see Fig. 1) or surface relief structures [9]. Alternatively, as will be explained in Sect. 3, additional photons can be introduced into the cavity by a focused tunable laser beam. Functional devices can be processed with a few cleanroom steps, not requiring the critical wet-thermal oxidation. Thus, the problematic strain close to the active zone is eliminated, which could extend the lifetime of the VCSELs. Moreover, the optimized spatial overlap between the current and photon distribution could lead to more efficient lasers.

3. External Current Aperture Definition and Manipulation

To modify the location of the current aperture during the turn-on of the PT-VCSEL means to influence the spatial photon distribution in the resonator. This can be done by incrementing the number of photons via light injection. We employ an external tunable laser with an optical output power of up to 35 mW and a wavelength range from 990 to 1075 nm. The wavelength of these photons must be chosen according to the resonance dip in the reflection spectrum of the PT-VCSEL to ensure the best possible injection efficiency. Owing to the red-shift of the spectrum caused by internal heating, the wavelength of the external laser needs to be readjusted when changing the drive current.

To qualitatively investigate the influence of additional photons in the cavity of PT-VCSELs, we have grown a test sample by molecular beam epitaxy on an n-doped GaAs wafer. The resonator is formed by p- and n-doped AlGaAs/GaAs Bragg mirrors consisting of 29 and 26.5 layer pairs, respectively. The calculated threshold gain is 1522 cm^{-1},

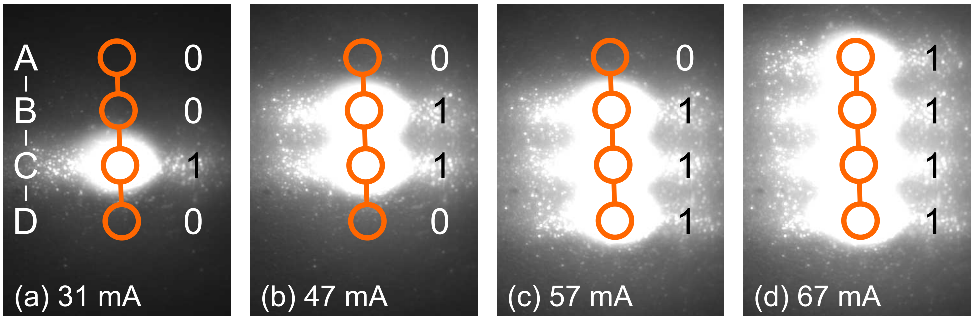

Fig. 3: CCD camera images of the bottom side of spontaneously emitting PT-VCSELs according to Fig. 2. The top metal contact structure is highlighted in orange. "0" and "1" represent the off-/on-state of each PT, respectively, and the turn-on currents where the individual PTs become locally conductive are displayed at the bottom. As in Fig. 2 the needle contacts an outer ring at position D. The turn-on order is C–B–D–A.

and the absorption coefficient of the α-QW is estimated to be $\approx 3500\,\mathrm{cm}^{-1}$. To reach strong current confinement, the current gain β is kept very low [10], namely $\beta \approx 2$ in this sample.

We have processed one-dimensional arrays of four parallel-driven PT-VCSELs (see Fig. 2). Ti/Pt/Au contact rings on the surface with 100 µm inner diameter define each device. The rings are interconnected by 100 µm long metal lines with a width of 30 µm. The back side of the substrate was kept free from metal to guarantee an unobstructed view at the light output pattern of the PT-VCSEL. The sample holder has a dedicated opening for transmission of the bottom-emitted light. A large-area n-contact is established between the sample and the Au-coated vacuum holder. The current source is connected to the sample holder and to a tungsten needle which contacts the top metalization of device D. In addition to light versus current measurements, the setup allows to take CCD camera images from the bottom side of the wafer and obtain new insights about the turn-on process of the laser structure. Without external laser illumination, the turn-on order of these samples always follows a consistent routine [11]. Figure 3 shows the camera images taken from the back side of the structure during the turn-on process. Ramping up the current, during dark-current operation (before 31 mA), there is an almost homogeneous current flow over the whole width of the structure, which already generates faint spontaneous emission in the active zone. Finally, at 31 mA the PT with the highest leakage current of the base–collector junction begins to open (here at position C). Subsequently, while further increasing the drive current, spontaneous photons reach the adjacent regions and successively turn these PTs on. At 67 mA, all four parallel-driven PT-VCSELs are switched into a conductive state and show spontaneous emission. For still higher currents the needle-contacted array begins to lase where owing to lateral ohmic losses the highest current density is reached.

To manipulate the turn-on order from Fig. 3, we repeat the experiment while focusing the external laser beam at different positions on the surface (see Fig. 2). The power of the laser was set to 6.4 mW and the wavelength was chosen as 1038 nm according to the reflection characteristics. Initially, the drive current was set to 25 mA to operate in

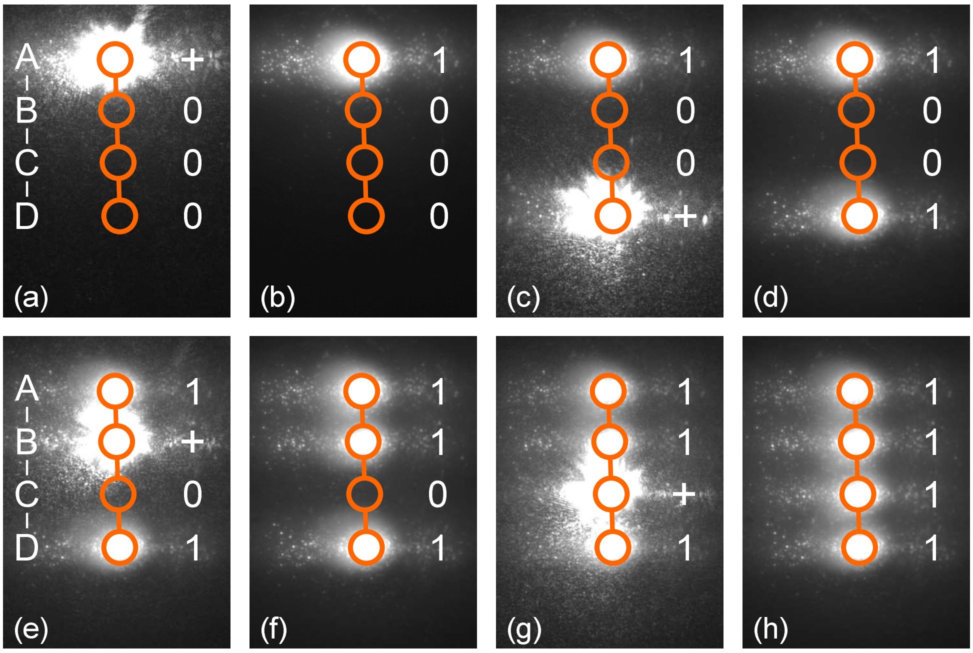

Fig. 4: CCD camera images of the bottom side of the PT-VCSEL arrangement from Fig. 2 at a constant current of 25 mA. The white "+" indicates the contact ring into which the external laser beam is focused. The images (a)–(h) illustrate a sequential experiment in which the external laser is switched on and off to open an additional PT. The stray light in the vicinity of the position "+" in images (a), (c), (e), and (g) originates from external laser emission transmitted through the complete device. The turn-on order of the one-dimensional array can be changed in any arbitrary way (here: A–D–B–C).

the dark-current mode of the PT-VCSELs. After directing the external laser beam to position A of the contact structure, the additional injected photons turned this PT into a conductive state even after switching the laser off again. As proven by Fig. 4, the turn-on order now exclusively depends on the position of the laser beam. Since the drive current is kept constant during the entire experiment, the turn-on current of the PTs was consequently decreased compared to the results in Fig. 3.

4. Impact of External Power and Wavelength

During the previous investigations, the optical power and wavelength of the external laser beam were kept constant. However, since the amount of injected photons is crucial for the turn-on of the PT-VCSEL, the output power of the external laser consequently has a direct influence on the device behavior. The impact of the photon wavelength depends strongly on the temperature-dependent emission spectrum of the PT-VCSEL. For functional devices it is essential to design the resonator and the α-QW in the same wavelength range. Since the diameter of the focused external laser beam is about 60 µm, a large-diameter PT-VCSEL device with 230 µm metal contact opening was chosen for the light–current (LI) measurements. This size is a compromise between small-diameter and large-area devices. On the one hand, in small devices, the large laser spot size would

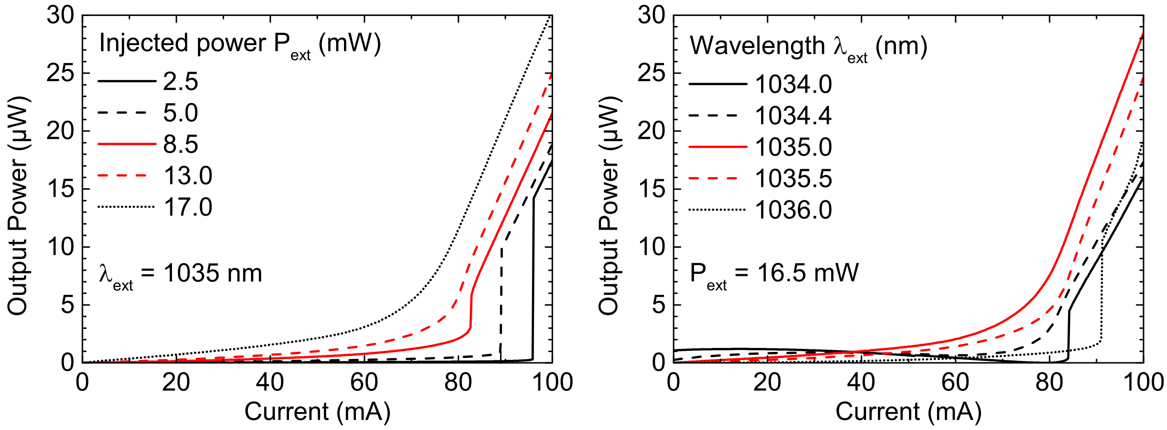

Fig. 5: Measured LI curves of a bottom-emitting PT-VCSEL with a contact ring diameter of 230 µm while varying the injected optical power (left) and the wavelength of the external laser source (right).

switch the whole mesa conductive, which would result in mesa current confinement. On the other hand, oversized samples are problematic owing to the higher ohmic resistance of the long lateral current paths between contact ring and current aperture. Figure 5 (left) depicts the LI measurements for different optical input powers P_{ext} from the external laser. The wavelength is kept constant to $\lambda_{ext} = 1035$ nm. It is obvious that the turn-on current of the PT (determined by the step-like rise of output power) decreases while intensifying the illumination, namely more photons per time are incorporated into the resonator, which helps to reach the threshold base current at lower drive currents. Also, instead of a step-like behavior, the LI curves show a more and more gradual onset of lasing operation. The step results from a sudden transition from an insulating to a conductive state of the PT. Simultaneously, the majority of carriers funnel through the newly established optically defined current aperture, which increases abruptly the current density and leads to a higher photon generation until finally stimulated emission is reached. This step is also detectable in the current–voltage (IV) characteristics, indicated as a sharp negative differential resistance region. By incorporating more external photons into the resonator, at some point (here between 8.5 and 13.0 mW) the PT switches conductive before the lasing threshold current density is reached. In this case the drive current must be further increased to reach lasing, which results in a smooth continuous LI curve and a diode-like IV characteristic. The decrease of the lasing threshold current with increasing input power can be explained by the accumulation of carriers in the α-QW as a result of absorption and the subsequent reduction of the absorption coefficient α from (1) (bleaching effect). Lower internal losses in the resonator then raise the slope of the LI curve. Concurrently, more external laser light can propagate through the device, which is detected by the optical power meter on the bottom side.

The influence of changes of the external laser wavelength λ_{ext} on the LI curve of the PT-VCSEL is illustrated in Fig. 5 (right). The external laser power was kept constant at 16.5 mW. The wavelength range for this investigation was chosen to be smaller than 1040 nm to ensure absorption of photons in the α-QW. Starting with 1034 nm (thus blueshifted to Fig. 5 (left)) the already known step function in the LI graph appears again (it disappeared at 13 mW already in the left figure part). Since λ_{ext} is outside the resonance dip of the laser at around 1035 nm, more photons of the external laser are reflected at the top surface and do no affect the turn-on process at 84 mA. However, they partly enter the resonator in the $0 \ldots 30$ mA drive current region and already create a current aperture. This effect is noticeable in the local maximum of the output power at about 15 mA caused by transmitted external laser light through the device, which is also responsible for finite light detection at zero current. While further increasing the current (and therefore red-shifting the spectrum), the influence of the external laser almost disappears again and the internally (in the active layers) generated photons at these low drive currents still do not suffice to keep the aperture open. This is the case only at 84 mA, as indicated by the step in the LI curve. By slightly increasing λ_{ext}, more external photons are injected at higher VCSEL currents. At 1035 nm the resonance dip of the PT-VCSEL is at the perfect position — leading to low turn-on currents — to support the establishment of the current aperture and subsequently keeping it open only by internally generated photons, even when the external amount of photons decreases while further increasing the current (and red-shifting the spectrum). Raising the wavelength to 1036 nm, the external photons cannot influence the turn-on process because they are able to enter the resonator only at high drive currents after the turn-on of the PT already happened internally. These measurements give valuable insight into the the turn-on behavior of PT-VCSELs and demonstrate the difficulty to mutually adjust the injection wavelength, the power, and the drive current to minimize the turn-on and lasing threshold currents.

5. Conclusion and Outlook

We have discussed the concept of optically controlled current confinement in VCSELs that contain a phototransistor in the cavity. We have presented detailed studies about the optical manipulation of the current aperture in PT-VCSELs by using a tunable laser beam. The possibility of externally defining the location of the current aperture in parallel-driven structures has been demonstrated. We have also investigated the impact of varying the optical power and wavelength of the external laser on the turn-on behavior of the PT-VCSELs and were capable to shift the turn-on current of the PT towards lower values without changing the current gain of the PT. The new insights help to optimize the next generation of PT-VCSELs regarding the turn-on characteristics as well as to motivate future PT-integrated devices like light-emitting diodes which could possibly be controlled by an external light source.

Acknowledgment

The authors thank Philips Photonics GmbH for the project support and the MBE growth of the PT-VCSEL wafer. Furthermore the authors are grateful to Dr.-Ing. Philipp Gerlach for many superb discussions and the fruitful cooperation. The technical assistance of Susanne Menzel and Rudolf Rösch in the cleanroom is highly appreciated.

References

[1] R. Michalzik (Ed.), *VCSELs — Fundamentals, Technology and Applications of Vertical-Cavity Surface-Emitting Lasers*, Springer Series in Optical Sciences, vol. 166, Berlin: Springer-Verlag, 2013.

[2] D.L. Huffaker, D.G. Deppe, K. Kumar, and T.J. Rogers, "Native-oxide defined ring contact for low threshold vertical-cavity lasers", *Appl. Phys. Lett.*, vol. 65, pp. 97–99, 1994.

[3] B.M. Hawkins, R.A. Hawthorne III, J.K. Guenter, J.A. Tatum, and J.R. Biard, "Reliability of various size oxide aperture VCSELs", in Proc. *52nd Electron. Comp. and Technol. Conf., ECTC 2002*, pp. 540–550. San Diego, CA, USA, May 2002.

[4] J.L. Jewell, A. Scherer, S.L. McCall, Y.H. Lee, S. Walker, J.P. Harbison, and L.T. Florez, "Low-threshold electrically pumped vertical-cavity surface-emitting microlasers", *Electron. Lett.*, vol. 25, pp. 1123–1124, 1989.

[5] M. Orenstein, A.C. Von Lehmen, C. Chang-Hasnain, N.G. Stoffel, J.P. Harbison, L.T. Florez, E. Clausen, and J.E. Jewell, "Vertical-cavity surface-emitting InGaAs/GaAs lasers with planar lateral definition", *Appl. Phys. Lett*, vol. 56, pp. 2384–2386, 1990.

[6] M. Ortsiefer, W. Hofmann, J. Rosskopf, and M.C. Amann, "Long-Wavelength VCSELs with Buried Tunnel Junction", Chap. 10 in *VCSELs*, R. Michalzik (Ed.), pp. 321–351, Berlin: Springer-Verlag, 2013.

[7] X. Yang, M. Li, G. Zhao, Y. Zhang, S. Freisem, and D. Deppe, "Small-sized lithographic single-mode VCSELs with high power conversion efficiency", in *Vertical-Cavity Surface-Emitting Lasers XIX*, C. Lei, K.D. Choquette (Eds.), Proc. SPIE 9381, pp. 93810R-1–6, 2015.

[8] S. Bader, P. Gerlach, and R. Michalzik, "Optically controlled current confinement in vertical-cavity surface-emitting lasers", *IEEE Photon. Technol. Lett.*, vol. 28, pp. 1309–1312, 2016.

[9] H.J. Unold, S.W.Z. Mahmoud, R. Jäger, M. Grabherr, R. Michalzik, and K.J. Ebeling, "Large-area single-mode VCSELs and the self-aligned surface relief", *IEEE J. Select. Topics Quantum Electron.*, vol. 7, pp. 386–392, 2001.

[10] S. Bader, P. Gerlach, and R. Michalzik, "VCSELs with optically controlled current confinement: experiments and analysis", in *Semiconductor Lasers and Laser Dynamics VII*, K.P. Panajotov, M. Sciamanna, A.A. Valle, R. Michalzik (Eds.), Proc. SPIE 9892, pp. 989208-1–6, 2016.

[11] S. Bader, P. Gerlach, and R. Michalzik, "Optically controlled current confinement in parallel-driven VCSELs", in Online Digest *Conf. on Lasers and Electro-Optics, CLEO/Europe 2017*, paper CB-3.4, one page. Munich, Germany, June 2017.